

## Article

# Using Ground- and Drone-Based Surface Emission Monitoring (SEM) Data to Locate and Infer Landfill Methane Emissions

Tarek Abichou <sup>1,\*</sup>, Nizar Bel Hadj Ali <sup>2</sup> , Sakina Amankwah <sup>1</sup>, Roger Green <sup>3</sup> and Eric S. Howarth <sup>4</sup>

<sup>1</sup> FAMU-FSU College of Engineering, Florida State University, Tallahassee, FL 32310, USA; sakina.amankwah@famu.edu

<sup>2</sup> Ecole Nationale d'Ingénieurs de Gabès, University of Gabès, Gabès 6029, Tunisia; nizar.belhadjali@enig.rnu.tn

<sup>3</sup> Waste Management, Houston, TX 77002, USA; rgreen2@wm.com

<sup>4</sup> Technical Field Support, Florida State University, Tallahassee, FL 32310, USA; ehowarth@fsu.edu

\* Correspondence: abichou@eng.famu.fsu.edu; Tel.: +1-850-410-6661

**Abstract:** Ground- and drone-based surface emission monitoring (SEM) campaigns were performed at two municipal solid waste landfills, during the same week as mobile tracer correlation method (TCM) testing was used to measure the total methane emissions from the same landfills. The G-SEM and the D-SEM data, along with wind data, were used as input into an inverse modeling approach combined with an optimization-based methane emission estimation method (implemented in a tool called SEM2Flux). This approach involves the use of backward dispersion modeling to estimate the whole-site methane emissions from a given landfill and the identification of locations and emission rates of major leaks. SEM2Flux is designed to exploit the measured surface methane concentration concurrently with wind data and tackle two problems: (1) inferring the estimates of methane rates from individual landfills, and (2) identifying the likely locations of the main emission sources. SEM2Flux results were also compared with emission estimates obtained using TCM. In Landfill B, the average TCM-measured methane emissions was 1178 Kg/h, with a standard deviation of 271 Kg/h. In Landfill C, the average TCM-measured emission rate was 601 Kg/h, with a standard deviation of 292 Kg/h. For both landfills, the D-SEM data yielded statistically similar estimates of methane emissions as the TCM-measured emissions. On the other hand, the G-SEM data yielded comparable estimates of emissions to TCM-measured emissions only for Landfill C, where the D-SEM and G-SEM data were statistically not different. The results of this study showcase the ability of this method using surface concentrations to provide a rapid and simple estimation of fugitive methane emissions from landfills. Such an approach can also be used to assess the effectiveness of different remedial actions in reducing fugitive methane emissions from a given landfill.

**Keywords:** methane emission monitoring; landfill emissions; tracer correlation method; SEM; drones



**Citation:** Abichou, T.; Bel Hadj Ali, N.; Amankwah, S.; Green, R.; Howarth, E.S. Using Ground- and Drone-Based Surface Emission Monitoring (SEM) Data to Locate and Infer Landfill Methane Emissions. *Methane* **2023**, *2*, 440–451. <https://doi.org/10.3390/methane2040030>

Academic Editor: Patrick Da Costa

Received: 27 October 2023

Revised: 19 November 2023

Accepted: 5 December 2023

Published: 11 December 2023



**Copyright:** © 2023 by the authors. Licensee MDPI, Basel, Switzerland. This article is an open access article distributed under the terms and conditions of the Creative Commons Attribution (CC BY) license (<https://creativecommons.org/licenses/by/4.0/>).

## 1. Introduction

Attention to methane emissions from all sources, including landfills, is significantly increasing. This is due to methane's high global warming potential, which is 84 times that of carbon dioxide over a 20-year period. Methane concentrations in the atmosphere have risen by more than 50% since preindustrial times, posing significant threats to the environment and global development [1].

The decomposition of organic materials in landfills under anaerobic conditions ranks as the third-largest source of methane emissions in the United States, trailing behind enteric fermentation and natural gas systems [2]. Municipal solid waste (MSW) landfills contributed to 17% of the total methane emissions in the US in 2021 [2]. Quantifying the amount of fugitive methane emissions is very important in the efforts to report greenhouse gas emissions at the facility level. Reducing fugitive methane emissions from landfills stands as a critical element of greenhouse gas mitigation. To accomplish this goal, it is imperative to closely monitor landfills to ensure compliance with environmental protection

regulations, which includes monitoring fugitive gases like methane. This task entails two fundamental steps: firstly, employing efficient and precise methods for detecting and estimating landfill methane emissions, and secondly, but equally important, leveraging these measurement data to plan remedial actions and to quantify and monitor the pre-and post-remediation activities of methane emission rates.

As for landfill methane measurement, a wide range of methods have been successfully deployed during the few past decades [3]. Measurement techniques vary from point/local assessment to aerial/global surveys [4]. Closed and open surface flux chambers are historically the most used methods to perform single-point methane measurement. However, this method is not appropriate for whole-site methane emission quantification [5]. Downwind cross-plume scanning through radial plume mapping (RPM) coupled with wind measurement can be used to measure emission fluxes [6]. RPM uses optical remote sensing (ORS) by means of laser infrared radiation emissions [7]. Recently, the mass balance approach has been applied using aircraft and unmanned aerial vehicles (UAVs) [8,9]. In this method, atmospheric methane concentration measurements across the downwind plume at several heights are employed to generate a vertical plane concentration profile. Combined with wind data, measured methane mass is used to estimate the emission rate. Methodologies for measuring landfill methane emissions also include the tracer correlation method [10]. This method relies on the controlled release of a tracer gas on top of the landfill and subsequent downwind measurements of both methane and the tracer gas. The total methane emission from landfills can be calculated by correlating downwind concentrations with the known emission rate of the tracer gas. More recently, satellite-based remote sensing techniques are increasingly being used and deployed, taking advantage of innovative methane-specific detection instruments [11].

In the US, landfill operators are required to perform surface emission monitoring (SEM) campaigns on landfill surfaces to identify and remediate high-emitting zones quarterly. Such regulations caused SEM data to become the most abundant data related to methane emissions in US landfills. Surface emission monitoring (SEM) can be performed by employing walking-based measurements (using FID or equivalent equipment) or by employing newer methodologies and technical advances offered through UAVs such as drones [12–14]. Ground-based (G-SEM) campaigns are performed using relatively affordable equipment. However, scanning large areas can be time-consuming and may take several days. In addition, G-SEM is limited to accessible parts of the landfill. In contrast, drone-based (D-SEM) campaigns allow for the monitoring of difficult-to-access locations at a given landfill. Furthermore, D-SEM allows for faster methane emission monitoring and a larger sampling density as compared to G-SEM.

With the abundance of SEM data arises the question of how to make better use of surface concentration measurements to locate emission sources and infer an estimate of methane emissions at the monitored landfills, in other words, how to transform measured methane concentrations (in ppmv) to an estimate of the emission rate (in Kg/h). Some researchers tried to establish simple correlation equations linking surface methane concentrations to emission rates [12,13]. Ref. [15] used ambient air volatile organic compound (VOC) measurements and Voronoi diagrams to predict the locations of potential methane emission sources. Emission rates were then calculated using linear regression. Refs. [16,17] used inverse plume modeling to estimate the whole-site methane emissions from a given landfill. The proposed method was also used to identify high-emitting zones and emission rates of major leaks.

The proposed method in this study builds upon previous work by Bel Hadj Ali et al. [16] consisting of an inverse modeling approach combined with an optimization-based methane emission estimation method. The fugitive methane emission estimation method was implemented using SEM2Flux [16]. SEM2Flux is a tool implemented in Matlab<sup>®</sup> (R2020a, MATLAB 9.8) and designed with a graphical user interface. The method exploits measured surface methane concentration, simultaneously with wind data, to tackle two objectives: inferring the estimates of methane rates and identifying the likely locations

of the main emission sources. The G-SEM and D-SEM data were collected during the same period when tracer correlation method (TCM) campaigns were performed at the two landfill sites. This allowed for comparing estimates obtained through the SEM2Flux tool with those obtained using the TCM approach. The remainder of the paper is organized as follows: In Section 2, the main findings of the study are presented and discussed. In Section 3, the studied landfills, fieldwork, and data collection are described. Section 3 also includes a presentation of the main outlines of the SEM2Flux methodology. Finally, the study's main results and conclusions are presented in Section 4.

## 2. Results

As will be described in the Methods section, the fieldwork was performed at two active municipal waste disposal sites located in Southeast, USA (Landfill B and Landfill C). Three different monitoring methods were employed at each landfill during the same period: ground-based SEM (G-SEM), drone-based SEM (D-SEM), and mobile tracer correlation method (TCM). The measurement campaigns were carried out in 5 days at the two landfills. Figures 1 and 2 show the serpentine path and the sampling points of the G-SEM and the D-SEM data for both landfills. Note that the G-SEM and the D-SEM data were obtained by different operators. Figures 1 and 2 showcase the difference in the sampling density of G-SEM versus D-SEM. G-SEM data collection required multiple days as opposed to D-SEM data collection. Figures 1 and 2 show that the extent of the area being sampled was designed to cover the entire waste footprint. The different colors in Figures 1 and 2 correspond to the data collected on different days.

### 2.1. SEM Data Characteristics

Table 1 shows the summary statistics for the SEM collected data. For each dataset, the maximum, minimum, median, mean, and standard deviation of methane concentrations are presented in Table 1. The total number of readings, the surface area occupied by the data, and the number of measurements exceeding 500 ppmv (exceedances) are also shown in Table 1. Note that the background concentration (1.9 ppmv) was subtracted from all measured methane concentrations prior to any statistical treatment.

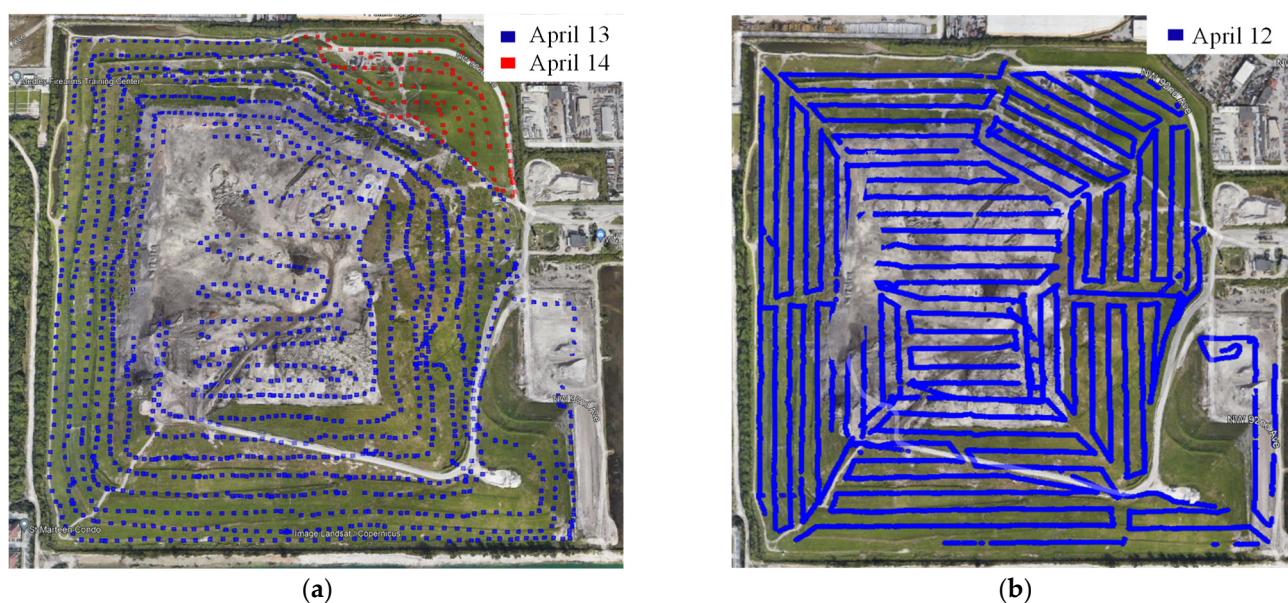


**Figure 1.** (a) G-SEM data for Landfill B; (b) D-SEM data for Landfill B.

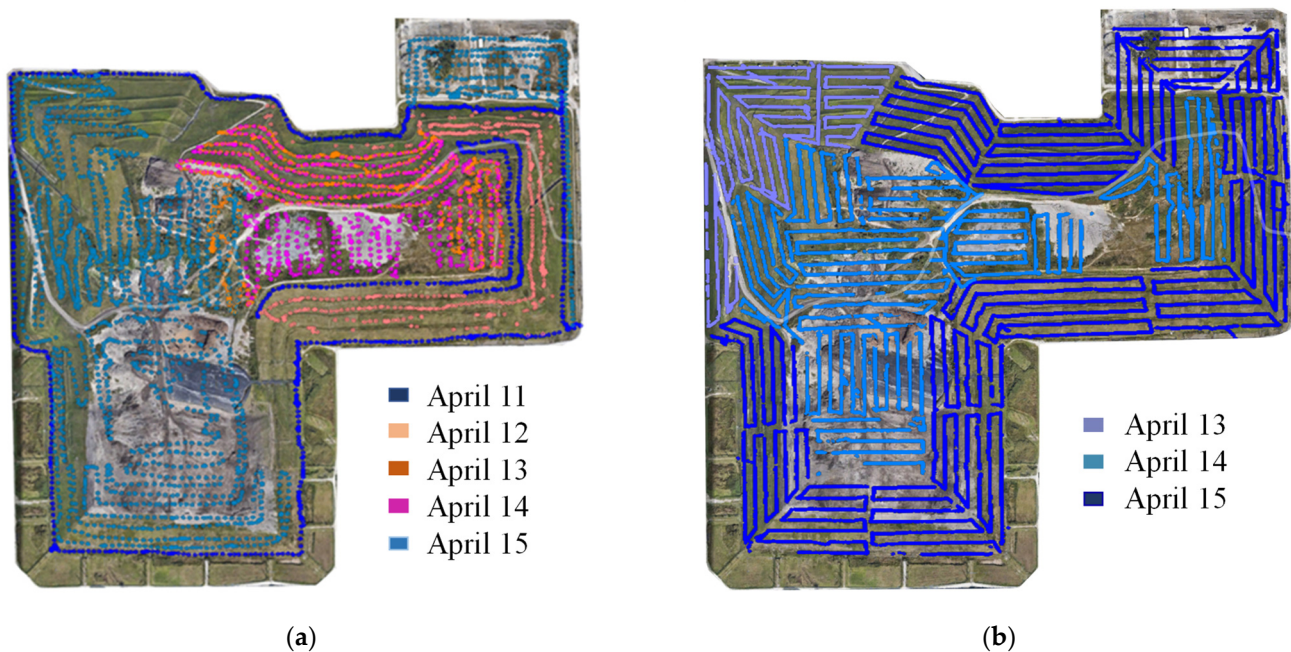


**Figure 2.** (a) G-SEM data for Landfill C; (b) D-SEM data for Landfill C (3 days because of drone technical issues).

**Table 1.** Summary statistics of collected SEM data.

Data Name	Dates	SEM Data (ppmv)							
		Max	Min	Median	Mean	Std Dev.	Count	Exce.	Area (Ha)
Landfill B Drone	12 April 2022	1603	0	26	55	90	23,398	98	62
Landfill B Ground	13–14 April 2022	279	0	0	9	24	1898	0	68
Landfill C Drone	14 April 2022	787	0	2	7	20	51,867	7	152
Landfill C Ground	14–16 April 2022	15,192	0	0	17	299	4894	21	152

In Landfill B, 23,398 surface methane concentrations were collected during the D-SEM campaign as opposed to 1898 during the G-SEM campaign. The mean (average) of the D-SEM data was 55 ppmv, with a standard deviation of 90 ppmv. The G-SEM data had a mean of 9 ppmv and a standard deviation of 24 ppmv. A *t*-test was used to better investigate the two measurement datasets. The calculated *t*-statistic was equal to 2.32. The *t*-test performed at a 95% confidence level (1.96) revealed a statistically significant difference between D-SEM and G-SEM datasets for Landfill B. This implies a statistically significant difference between the means of these two datasets.

For Landfill C, 51,867 surface methane concentrations were collected using the drone, as opposed to 4894 data points during the G-SEM campaign. The average methane concentration for the D-SEM campaign was 7 ppmv, with a standard deviation of 20, as opposed to 17 ppmv, with a standard deviation of 299 for the G-SEM data. Since the absolute value of the calculated *t*-statistic (0.0776) was less than 1.96, the null hypothesis was rejected when comparing the G-SEM and D-SEM datasets for Landfill C. Thus, at a 95% confidence level, the means of datasets were not significantly different.

Table 2 shows the density of surface concentration reading per hectare of the surveyed area. As expected, D-SEM allowed for sampling 10 to 13 times more points per hectare than G-SEM. Note that the G-SEM spacing is dictated by the maximum spacing between the walking path of the G-SEM operator (30 m). D-SEM allowed for a rapid survey of the landfill and provided a larger number of concentration measurements compared with

G-SEM. Table 2 shows the distributions of the surface concentration data from the G-SEM and the D-SEM campaigns from both landfills.

**Table 2.** Distribution of D-SEM and G-SEM data collected at Landfills B and C \*.

Data Name	Data Density (Number/Hectare)	>500 ppmv	200 to 499 ppmv	100 to 199 ppmv	1 to 100 ppmv	0 ppmv
Landfill B D-SEM	376	98 (0.42)	1359 (5.81)	2438 (10.42)	11,169 (47.73)	8146 (34.81)
Landfill B G-SEM	28	0 (0)	4 (0.21)	24 (1.26)	628 (33.09)	1241 (65.38)
Landfill C D-SEM	340	7 (0.01)	90 (0.17)	262 (0.51)	26,933 (51.93)	23,424 (45.16)
Landfill C G-SEM	32	21 (0.43)	21 (0.43)	41 (0.84)	1828 (37.35)	2983 (60.95)

\* All numbers in parentheses are %.

Table 2 shows the number and the percentile readings higher than 500 ppmv, which are considered “exceedances” by the SEM regulations. Exceedances are likely to be caused by leaks in the gas collection system or defects or cracks in the soil cover. The SEM regulations require that areas with exceedances be remediated until surface methane concentrations fall below 500 ppmv. For Landfill B, D-SEM data resulted in the identification of 98 (0.42%) exceedances in need of remediation. Surprisingly, G-SEM performed at Landfill B contained no exceedances. For Landfill C, 7 (0.01%) exceedances were identified with the D-SEM data, and 21 (0.43) exceedances were identified with the G-SEM data.

The D-SEM data for both landfills consisted of 34.81% to 45.16% of zero ppmv (above background). The G-SEM data consisted of 60.95% to 65.38% of zero ppmv (above background). The D-SEM data for both landfills consisted of 47.73% to 51.93% of 1 to 100 ppmv (above background). The G-SEM data consisted of 33.09% to 37.35% of 1 to 100 ppmv (above background). Therefore, the D-SEM data consisted of 83% to 97% of readings below or equal to 100 ppmv. The G-SEM data consisted of 98% of readings below or equal to 100 ppmv (above background). For all four SEM data, the majority of the data consisted of methane concentrations (above background) below 100 ppmv.

## 2.2. SEM2Flux™ Results

The measurement datasets obtained using G-SEM and D-SEM, along with wind speed and wind direction measurements, were used as input using an inverse modeling approach to determine the independent estimates of total methane emissions from Landfills B and C, using the SEM2Flux tool, as described later in the Methods section. The output of SEM2Flux corresponds to the optimal solution (source intensity and location) that represents the best fit between measured and modeled concentrations. The search for the optimal source configuration terminates when there is no improvement in the fitness of the source configuration for a certain number of iterations. Three SEM2Flux runs were performed for each G-SEM and D-SEM dataset. The results of the three simulations were used to provide the average and standard deviations of total landfill fugitive methane emission rates. Additionally, the SEM2Flux tool also yielded locations of major methane emitting zones on the landfill and their individual emission rates in grams/second (g/s). Table 3 shows the results of the SEM2Flux simulations.

**Table 3.** Summary of SEM2Flux simulations for Landfills B and C.

Data Name	Date	N. Major Sources	SEM2Flux Emission Results	
			Total Fugitive Emissions (Kg/h)	StDev (Kg/h)
Landfill B D-SEM	12 April 2022	30	1309	331
Landfill B G-SEM	13–14 April 2022	12	531	75
Landfill C D-SEM	14 April 2022	15	657	214
Landfill C G-SEM	14–16 April 2022	12	573	99

Thirty major methane emission sources were identified with SEM2Flux using the D-SEM data collected from Landfill B. The 30 sources identified with SEM2Flux correspond to an average total landfill fugitive emissions of 1309 Kg/h and a standard deviation of 331 Kg/h. The G-SEM data, on the other hand, yielded only 12 major emission sources, corresponding to an average total fugitive emission rate of 531 Kg/h and a standard deviation of 75 Kg/h. As expected, the G-SEM and the D-SEM data yielded statistically different total fugitive emission rates because the actual data were shown to be statistically different, as stated in the previous section.

For Landfill C, 15 and 12 major methane emission sources were identified with SEM2Flux using D-SEM and G-SEM data, respectively. The total fugitive emission rate estimated with SEM2Flux using D-SEM data was 675 Kg/h, with a standard deviation of 214 Kg/h, and 573 Kg/h, with a standard deviation of 99 Kg/h using G-SEM data. In Landfill C, the SEM2Flux results of G-SEM and D-SEM data were not significantly different.

Figure 3 shows the locations of the major methane emission sources as determined with SEM2Flux using D-SEM for Landfill B and Landfill C. Figure 3a suggests that, for Landfill B, the G-SEM data failed to identify some areas on the landfill responsible for the majority of emissions (blue triangles) as opposed to the sources determined with the D-SEM data (red squares). The red squares seem to be located in the central area of the landfill. As for Landfill C, the G-SEM and D-SEM yielded generally sources in the same northeast corner of the landfill. The SEM2Flux results from G-SEM data simulations demonstrate that the emission sources identified at the northeast corner of Landfill C are responsible for 85.6% of the total methane emitted at the entire landfill. When D-SEM data were employed, the results showed that the sources that were identified in the same zone contributed to approximately 81% of the total estimated methane flux.

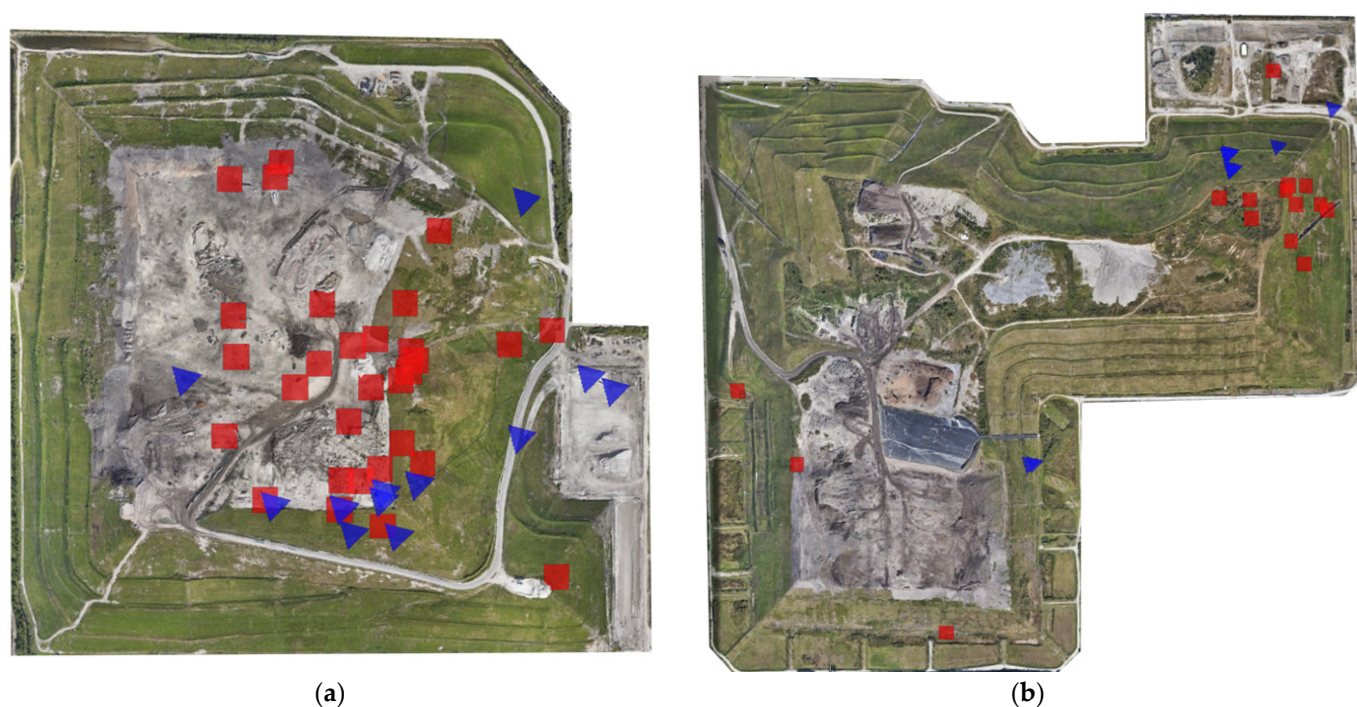


**Figure 3.** Locations of major methane emission sources as predicted with SEM2Flux (red squares using D-SEM data, blue triangles using G-SEM data): (a) Landfill B; (b) Landfill C.

### 2.3. Comparison of SEM2Flux™ Results and Tracer Correlation Method (TCM)

As described in the Methods section, tracer correlation method (TCM) testing was performed during the same week as the D-SEM and G-SEM data collection campaigns. The tracer correlation method is considered the most reliable technique for estimating emission rates in landfills and is often used to provide ground truth data for other technologies

or techniques. Table 4 shows the summary of the TCM estimates of fugitive methane emissions from both of the landfills during the monitoring period. Twenty estimates of methane emissions were obtained in Landfill B over the monitoring campaign. The average TCM-measured methane emissions for Landfill B was 1178 Kg/h, with a standard deviation of 271 Kg/h. In Landfill C, 16 measurements of methane emissions were obtained during the monitoring period. The average TCM-measured emission rate for Landfill C was 601 Kg/h, with a standard deviation of 292 Kg/h. Figure 4 shows the TCM-reported emissions plotted with emission estimates as predicted with SEM2Flux using the G-SEM and D-SEM data. For both landfills, the D-SEM data yielded statistically similar estimates of methane emissions as the TCM-measured emissions. On the other hand, the G-SEM data yielded comparable estimates of emissions to TCM-measured emissions only for Landfill C, where the D-SEM and G-SEM data were statistically not different.

**Table 4.** Summary of TCM results.

Tracer Correlation Testing Data			
Date	TCM Emissions (Kg/h)	n	StDev (Kg/h)
11–13 April 2022	1178	23	271
14–16 April 2022	601	16	292

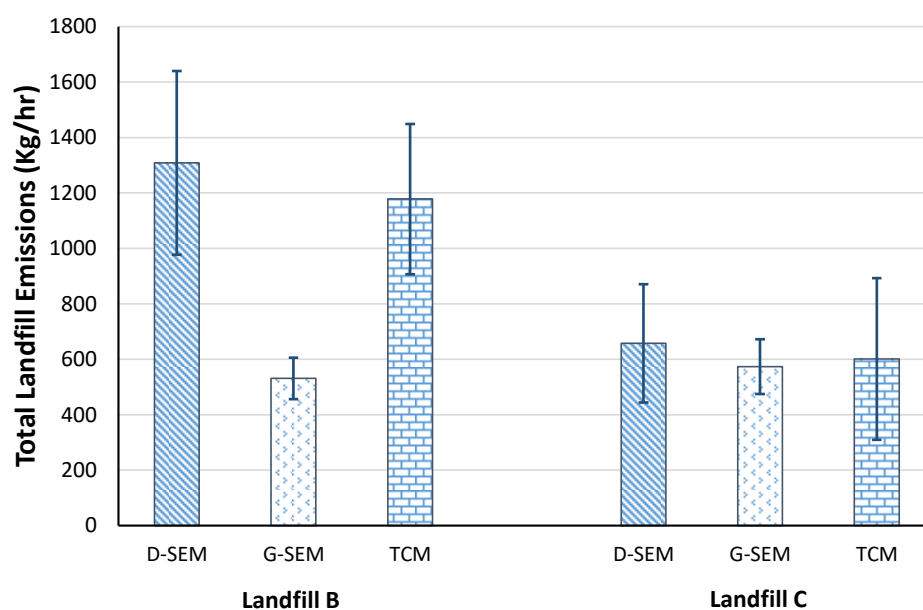


**Figure 4.** Comparison of fugitive methane emissions as estimated with SEM2Flux using D-SEM and G-SEM data and those measured with TCM.

### 3. Materials and Methods

#### 3.1. Fieldwork and Data Collection

The studied landfills are active municipal waste disposals (located in FL, USA). A ground-based monitoring campaign (G-SEM), a drone-based air monitoring campaign (D-SEM), and a mobile tracer correlation monitoring campaign (TCM) were conducted at the two studied landfills during the time same period. All fieldwork data were collected between 11 and 16 April 2022. An ultrasonic anemometer (Model 81000V from Young, Inc., Traverse City, MI, USA) was installed at an elevation of 2 m from the ground during the field measurement campaigns to measure wind speed, with a precision of 0.01 m/s and an accuracy of  $\pm 0.05$  m/s. The anemometer was located at the highest elevation of the landfill, next to one of the tracer release points used for TCM testing. The wind direction measurements precision was 0.1 degrees, with an accuracy of  $\pm 2$  degrees. The wind data

collected with a field-installed anemometer was used with the G-SEM data only. For D-SEM, wind speed and wind direction were collected using the drone itself. Wind velocities and direction were collected during the flight from the drone scan data via an algorithmic developed for determination of wind data from the rotor power of Sniffer Robotics drone. The drone is programmed to measure methane concentrations on the surface of a landfill while flying at a specific elevation above the landfill surface.

The field testing campaign lasted 4 days of data collection. The TCM testing consisted of 3 to 4 days (daytime only) of the continuous release of acetylene and downwind plume monitoring at distances varying from 1.5 to 2.5 Km from the landfill. The data from all three days were then averaged as an estimate of total emissions from the landfill during the 3–4 days of measurements. The ground- and drone-based SEM data consist of ppmv above the background concentration, which is typically 1.9 ppmv.

Ground-based surface monitoring was performed using a portable Flame Ionization Detector (MicroFID from PhotoVac, Inc. (Waltham, MA USA) with readings performed every 15 s. The MicroFID was calibrated at the beginning of each monitoring event, in accordance with the USEPA regulations. Ground-level methane concentrations were collected via an integrated pump, and the emitted gas was drawn using the MicroFID. A GPS unit registered measurement positions along the monitoring path.

Drone-based air monitoring (D-SEM) was performed by Sniffer Robotics, LLC (Ann Arbor, MI USA), following a test procedure that was approved by the US EPA. The test method is designed to automate the ground-based SEM by using a methane detection payload onboard an unmanned aerial system (UAS) coupled with a ground-level UAS sampling system. Methane samples were collected through the nozzle inlet placed within 5–10 cm of the ground. The geolocated methane readings were transmitted from the drone to the operator via a wireless communication system. During the D-SEM test, the flying height of the drone was continuously measured from the ground surface and was kept constant at 6 m above the ground surface.

In addition to the G-SEM and D-SEM tests, a tracer correlation method (TCM) was used for quantifying methane emissions from the two landfills. TCM is a remote sensing method that involves releasing a tracer gas at a specific rate at the source area. Methane and tracer gas concentrations are then measured simultaneously. Measurements are to be performed downwind of the emitting area following a sampling path that should preferably be perpendicular to the wind direction and sufficiently far (1 to 3 km) from the emitting area. From the well-mixed plume of both gases, as measured downwind from the landfill, the methane emission rate of the landfill can be retrieved directly using a ratio method. The downwind concentrations of methane and the tracer gas (acetylene) were measured simultaneously by employing a mobile cavity ring-down spectrometer (CRDS). Several downwind traverses were performed during the monitoring period for each landfill. Mobile downwind plume measurements were performed using a CRDS Picarro G2203 Analyzer for methane and acetylene. The CRDS measures methane and acetylene in ppb levels. The precision of the CRDS is 3 ppb for methane and less than 600 ppt for acetylene. The CRDS was mounted in an SUV fitted with an external snorkel intake for gas sample collection at an elevation of around 2 m from the ground surface. Methane and tracer concentration measurements and GPS positions were recorded in a time-synchronized data file.

### *3.2. Proposed Methodology for Inferring Emission Rates from SEM Data*

The main idea behind the proposed methodology is to exploit ambient-air methane concentration measurements, widely collected during landfill surface emission monitoring (SEM) to identify major emission sources and to infer an estimate of the total methane emission of landfill sites. The methodology is based on a simplified approach using inverse dispersion modeling largely employed in environmental studies. Inverse plume modeling relies on the backward application of atmospheric dispersion equations in order to determine a pollutant emission flux based on a dataset of measured concentrations. The methodology is widely employed with a broad variety of measurement technologies

ranging from point/terrestrial to satellite-based sampling. The initiation of the proposed method is by obtaining the collected methane concentration data. Concentration measurements could be obtained through walking-based (G-SEM) campaigns or by using drones (D-SEM) equipped to make an equivalent measurement. Landfill surveys using drones are becoming more popular due to the simplicity offered by drone flights over landfill areas. G-SEM and D-SEM data were both used in this study.

In the proposed approach, input data include methane concentrations at specified locations in the studied landfill. Meteorological conditions during the measurement campaign are also usually known (wind speed, wind direction, insolation, and temperature). The collected concentration data were used to identify major emission sources through inverse dispersion modeling and optimization. High emitting zones in the landfill were also identified. This was achieved through tracing dispersed methane back to emission sources. This task was formulated as an optimization problem where the variables were the locations and the emission rates of the sources inside the landfill. The objective of this optimization task was to identify the configuration of emission sources (locations and leakage rates) that fit the best to the measured concentrations. The fitness of a defined configuration of sources was evaluated by calculating the corresponding methane concentrations at the same locations where measured concentrations are available. This was accomplished using an atmospheric dispersion model yielding a model-predicted value of methane concentration for each measurement location. The predicted concentration values are then compared with the actual measured methane concentrations. Hence, the performance of a source configuration was evaluated through the difference between the measured and predicted methane concentrations. The norm of absolute residuals calculated for all measurement points was the metric to be minimized in the optimization task.

The predicted methane concentrations were obtained using the Gaussian dispersion Equation (1). This equation models the dispersion of a nonreactive gaseous pollutant from an elevated point source. Equation (1) predicts the steady-state concentration (C) in  $\mu\text{g}/\text{m}^3$  at a point (x, y, z) located downwind from the source.

$$C(x, y, z) = \frac{Q}{2\pi u \sigma_y \sigma_z} \exp\left(-\frac{1}{2} \frac{y^2}{\sigma_y^2}\right) \left\{ \exp\left(-\frac{1}{2} \frac{(z-H)^2}{\sigma_z^2}\right) + \exp\left(-\frac{1}{2} \frac{(z+H)^2}{\sigma_z^2}\right) \right\} \quad (1)$$

In Equation (1), Q is the emission rate ( $\mu\text{g}/\text{s}$ );  $\sigma_y$  and  $\sigma_z$  (m) are the horizontal and vertical spread parameters that are functions of the along wind distance x and the atmospheric stability; u is the average wind speed at stack height (m/s); y is the crosswind distance from source to receptor (m); z is the vertical distance above the ground (m); and H is the effective stack height (the physical stack height plus the plume rise expressed in m).

In most cases, wind is measured at several meters above the ground. In fixed weather stations, wind measurements are usually performed at 2 m height above the ground. In the case of drone-based measurements, wind data are typically obtained at the drone flight elevation. Since the developed approach assumes ground sources, the wind speed at ground level needs to be calculated from the collected wind data. At the ground level, the logarithmic wind profile (Equation (2)) allows for estimating the vertical wind variation with height:

$$v_2 = v_1 \ln\left(\frac{h_2}{z_0}\right) / \ln\left(\frac{h_1}{z_0}\right) \quad (2)$$

In Equation (2), the reference wind speed  $v_1$  is the measured wind speed at height  $h_1$ ;  $v_2$  is the corrected wind speed at height  $h_2$ ; and  $z_0$  is the roughness length depending on land cover types.

The Gaussian dispersion equation uses relatively simple calculations requiring only two dispersion parameters ( $\sigma_y$  and  $\sigma_z$ ) to identify the variation in gas concentrations away from the diffusion source. Dispersion coefficients,  $\sigma_y$  and  $\sigma_z$ , are functions of wind speed, cloud cover, and surface heating by the sun. Generally, the evaluation of the diffusion

coefficients is based on atmospheric stability classes. In this study, the Pasquill–Gifford stability classes were employed, and dispersion coefficients were calculated using the Briggs model [17].

The core component of the proposed method was to identify the configuration of sources that fit the best to the measurement data. To this end, stochastic optimization was employed to explore the set of all possible configurations and progressively converge to the source configuration with the best fit to the measurement data. Source positions were generated inside the borders of the landfill. The corresponding emission fluxes were generated between 0 and an upper limit correlated with the highest measured concentration. The optimization task was performed using genetic algorithms (GAs): a global search method that belongs to the class of stochastic search algorithms [16].

The optimization procedure in GAs mimics the principles of natural evolution. Starting from an initial set of possible solutions, an iterative procedure yields new solutions using specific nature-inspired operators (selection, mutation, and crossover). Solutions that have higher fitness (i.e., better satisfy the optimization objectives) are identified, and these are given more opportunities to produce newer solutions. The GA algorithm evolves, in successive generations, changing the composition of the solution population, and thus enables convergence toward near-optimal global solutions. Through thousands of applications in various disciplines, GA techniques proved generally capable of traversing large and complex search spaces to provide near-optimal solutions.

#### 4. Summary and Conclusions

Ground- and drone-based surface emission monitoring (SEMs) campaigns were performed at two municipal solid waste landfills, during the same week as mobile tracer correlation method (TCM) testing was used to measure the total methane emissions from the same sites. The G-SEM and D-SEM data, along with wind data, were used as input using an inverse modeling approach combined with an optimization-based methane emission estimation method (SEM2Flux).

In addition to the measurement density differences between G-SEM and D-SEM, the statistical analysis of the measurement datasets showed that the means of the datasets could be significantly different even if measurement campaigns were performed in the same period. Statistical differences can help interpret the discrepancies observed in SEM2Flux results for Landfill B, where 30 major methane emission sources were identified using the D-SEM data as opposed to only 12 major emission sources identified using the G-SEM data.

In Landfill C, SEM2Flux results obtained using G-SEM data show that the emission sources identified at the northeast corner are responsible for 85.6% of the total methane emitted at the entire landfill. At this zone, emission sources identified using D-SEM data contribute to approximately 81% of the total estimated methane flux. These findings suggest that, based on the geographic distribution of the predicted sources, SEM2Flux can reveal high emitting zones at the studied landfills.

SEM2Flux results were also compared with emission estimates obtained using TCM. In Landfill B, the average TCM measured methane emissions was 1178 Kg/h, with a standard deviation of 271 Kg/h. In Landfill C, the average TCM-measured emission rate was 601 Kg/h, with a standard deviation of 292 Kg/h. For both landfills, the D-SEM data yielded statistically similar estimates of methane emissions as the TCM-measured emissions. On the other hand, the G-SEM data yielded comparable estimates of emissions to TCM-measured emissions only for Landfill C, where the D-SEM and G-SEM data were statistically not different. The results showcase the importance of the sampling density and the extent to which it could influence both emission quantification and high-emitting zone localization.

In addition, the comparison between TCM results and SEM2Flux predictions demonstrates that the SEM2Flux tool allows for the rapid and simple estimation of landfill methane emissions. This tool is promising when combined with both ground and drone SEM methods. Future research will involve an assessment of the ability of SEM2Flux to identify

locations of high emissions using controlled release studies, which will be performed by the research team.

**Author Contributions:** Conceptualization, T.A. and N.B.H.A.; methodology, T.A., R.G. and E.S.H.; software, T.A. and N.B.H.A.; validation, T.A. and N.B.H.A.; formal analysis, T.A. and N.B.H.A.; investigation, T.A. and N.B.H.A.; data curation, S.A.; writing—original draft preparation, T.A.; writing—T.A. and N.B.H.A.; visualization, T.A. and N.B.H.A.; supervision, T.A. and N.B.H.A.; project administration, T.A.; funding acquisition, T.A. All authors have read and agreed to the published version of the manuscript.

**Funding:** This research was funded by Environmental and Research and Education Foundation and Hinkley Center for Solid and Hazardous Waste Management.

**Institutional Review Board Statement:** Not Applicable.

**Informed Consent Statement:** Not Applicable.

**Data Availability Statement:** The authors confirm that the data supporting the findings of this study are available within the article. Interested parties can request data from the corresponding author.

**Acknowledgments:** We acknowledge Raami Abichou for making the graphs for this manuscript.

**Conflicts of Interest:** Author Roger Green was employed by the company Waste Management. The remaining authors declare that the research was conducted in the absence of any commercial or financial relationships that could be construed as a potential conflict of interest.

## References

1. Montzka, S.; The NOAA Annual Greenhouse Gas Index (AGGI). NOAA Global Monitoring Laboratory Website. 2022. Available online: <https://gml.noaa.gov/aggi/aggi.html> (accessed on 10 June 2023).
2. EPA. *U.S. Greenhouse Gas Emissions and Sinks: 1990–2021*; U.S. Environmental Protection Agency: Washington, DC, USA, 2023.
3. Mønster, J.; Kjeldsen, P.; Scheutz, C. Methodologies for measuring fugitive methane emissions from landfills—A review. *Waste Manag.* **2019**, *87*, 835–859. [[CrossRef](#)] [[PubMed](#)]
4. Sullivan, P.S.; Huff, R.H. The Evolution of Methane Emissions Measurements at Landfills: Where are We Now? In Proceedings of the A&WMA's 115th Annual Conference & Exhibition, San Francisco, CA, USA, 27–30 June 2022.
5. Castro Gámez, A.F.; Rodríguez Maroto, J.M.; Vadillo Pérez, I. Quantification of methane emissions in a Mediterranean landfill (Southern Spain). A combination of flux chambers and geostatistical methods. *Waste Manag.* **2019**, *87*, 937–946. [[CrossRef](#)] [[PubMed](#)]
6. Zhang, W.; Zhang, Y.; He, Y.; You, K.; Yu, D.; Xie, H.; Fan, B.; Lei, B. Quantifying gas emissions through vertical radial plume mapping with embedded radial basis function interpolation. *Measurement* **2023**, *217*, 113019. [[CrossRef](#)]
7. Thoma, E.; Green, R.; Hater, G.; Goldsmith, C.; Swan, N.; Chase, M.; Hashmonay, R. Development of EPA OTM 10 for Landfill Applications. *J. Environ. Eng.* **2010**, *136*, 769–776. [[CrossRef](#)]
8. Shah, A.; Allen, G.; Pitt, J.R.; Ricketts, H.; Williams, P.I.; Helmore, J.; Finlayson, A.; Robinson, R.; Kabbabe, K.; Hollingsworth, P.; et al. A Near-Field Gaussian Plume Inversion Flux Quantification Method, Applied to Unmanned Aerial Vehicle Sampling. *Atmosphere* **2019**, *10*, 396. [[CrossRef](#)]
9. Shaw, J.T.; Shah, A.; Yong, H.; Allen, G. Methods for quantifying methane emissions using unmanned aerial vehicles: A review. *Philos. Trans. R. Soc. A Math. Phys. Eng. Sci.* **2021**, *379*, 20200450. [[CrossRef](#)] [[PubMed](#)]
10. Scheutz, C.; Samuelsson, J.; Fredenslund, A.M.; Kjeldsen, P. Quantification of multiple methane emission sources at landfills using a double tracer technique. *Waste Manag.* **2011**, *31*, 1009–1017. [[CrossRef](#)]
11. Maasackers, J.D.; Varon, D.J.; Elfarsdóttir, A.; McKeever, J.; Jervis, D.; Mahapatra, G.; Pandey, S.; Lorente, A.; Borsdorff, T.; Foorthuis, L.R.; et al. Using satellites to uncover large methane emissions from landfills. *Sci. Adv.* **2022**, *8*, eabn9683. [[CrossRef](#)] [[PubMed](#)]
12. Olaguer, E.P.; Jeltema, S.; Gauthier, T.; Jermalowicz, D.; Ostaszewski, A.; Batterman, S.; Xia, T.; Raneses, J.; Kovalchick, M.; Miller, S.; et al. Landfill Emissions of Methane Inferred from Unmanned Aerial Vehicle and Mobile Ground Measurements. *Atmosphere* **2022**, *13*, 983. [[CrossRef](#)]
13. Lando, A.T.; Nakayama, H.; Shimaoka, T. Application of portable gas detector in point and scanning method to estimate spatial distribution of methane emission in landfill. *Waste Manag.* **2017**, *59*, 255–266. [[CrossRef](#)] [[PubMed](#)]
14. Abedini, A.R.; Atwater, J.W.; Ulrich, M.K. Quantifying Fugitive Methane Emission Rates from Municipal Landfills Based on Surface Methane Concentrations. In Proceedings of the Sardinia 2019, 17th International Waste Management and Landfill Symposium, Cagliari, Italy, 30 September–4 October 2019.
15. Mackie, K.R.; Cooper, C.D. Landfill gas emission prediction using Voronoi diagrams and importance sampling. *Environ. Model. Softw.* **2009**, *24*, 1223–1232. [[CrossRef](#)]

16. Bel Hadj Ali, N.; Abichou, T.; Green, R. Comparing estimates of fugitive landfill methane emissions using inverse plume modeling obtained with Surface Emission Monitoring (SEM), Drone Emission Monitoring (DEM), and Downwind Plume Emission Monitoring (DWPEM). *J. Air Waste Manag. Assoc.* **2020**, *70*, 410–424. [[CrossRef](#)] [[PubMed](#)]
17. Kormi, T.; Mhadhebi, S.; Bel Hadj Ali, N.; Abichou, T.; Green, R. Estimation of fugitive landfill methane emissions using surface emission monitoring and Genetic Algorithms optimization. *Waste Manag.* **2018**, *72*, 313–328. [[CrossRef](#)] [[PubMed](#)]

**Disclaimer/Publisher’s Note:** The statements, opinions and data contained in all publications are solely those of the individual author(s) and contributor(s) and not of MDPI and/or the editor(s). MDPI and/or the editor(s) disclaim responsibility for any injury to people or property resulting from any ideas, methods, instructions or products referred to in the content.